IJHEX

International Journal of Heat Exchangers
1524-5608/Vol VI(2005), pp.

Printed in U.S.A.

Rib fin effects on the overall equivalent heat transfer coefficient in a rib-roughened cooling channel

M.E. Taslim
Northeastern University, Boston, MA USA

(Received 11 October 2004; accepted 21 April 2005)

Rib-roughened cooling passages are commonly used in heat exchangers and in turbine airfoils to maintain acceptable metal temperatures in gas turbine high temperature environments. The presence of ribs on the heat exchanger walls and on the airfoil cooling walls introduces two heat transfer enhancing features- an increase in heat transfer area and a significant increase in heat transfer coefficients. Considerable amount of data are reported in open literature for the heat transfer coefficients both on the rib surface and on the floor area between the ribs. These studies cover some important geometric parameters such as the rib cross-sectional area, the rib angle with the flow direction, the rib height relative to the passage hydraulic diameter, the rib pitch-to-height ratio, the rib aspect ratio, etc. Many cooling design software tools, however, require an overall average heat transfer coefficient on a rib-roughened wall. For example, in an airfoil, dealing with a complex axial flow circuit in conjunction with 180° bends, numerous film holes, trailing-edge slots, tip bleeds, cross-over impingement, and a conjugate heat transfer problem, these tools often are not capable of handling the geometric details of the rib-roughened surfaces or local variations in heat transfer coefficient on a rib-roughened wall. On the other hand, assigning an overall area-weighted average heat transfer coefficient based on the rib and floor area and their corresponding heat transfer coefficients will have the inherent error of assuming a 100% "fin" efficiency for the ribs, i.e., assuming that rib surface temperature is the same as the rib base temperature. Depending on the rib geometry, this error could produce an overestimation of up to 20% in the evaluated rib-roughened wall heat transfer coefficient. In this paper, a correction factor is developed that can be applied to the overall area-weighted average heat transfer coefficient that, when applied to the ribbed wall's projection area, the net heat removal is the same as that of the rib-roughened wall. To develop this correction

factor, the experimental results of heat transfer coefficients on the rib and on the surface area between the ribs are combined with about 400 numerical conduction models to determine an overall equivalent heat transfer coefficient that can be used in cooling design software tools. The end result of this investigation is a correlation that encompasses most pertinent parameters including the rib geometry, rib fin efficiency, and the rib and floor heat transfer coefficients.

Key Words: Rib-Roughened Channels, Rib Fin Effects

---

1. INTRODUCTION

Cooling and heating channels in heat exchangers as well as serpentine cooling channels within turbine airfoils are usually roughened with ribs. These ribs increase the level of mixing of the cooler core air with the warmer air close to the channel wall and restart the boundary layer after flow reattachment between ribs resulting in enhanced convective heat transfer coefficients. Experimental results, reported by many investigators, show as high as a five-fold enhancement in heat transfer coefficients of rib-roughened surfaces when compared with those of smooth (non-ribbed) channels. Geometric parameters such as channel aspect ratio (AR), rib height-to-passage hydraulic diameter (e/D_h) or blockage ratio, rib angle of attack (α), the manner in which the ribs are positioned relative to one another (in-line, staggered, crisscross, etc.), rib pitch-to-height ratio (P/e) and rib shape (round versus sharp corners, fillets, rib aspect ratio (AR_{rib}), and skew ness towards the flow direction) have pronounced effects on both local and overall heat transfer coefficients. Considerable data are available on both the heat transfer coefficient on the passage surface between the ribs and on the rib surfaces. Some of these effects were studied by different investigators such as Abuaf et el. (1986), Burggraf (1970), Chandra (1987), Chandra and Han (1989), Han (1984), Han et al. (1978, 1985, 1992), Metzger et el. (1983, 1988, 1990), Taslim et el. (1988, 1994, 1996, 1998, 1999) and Webb et el. (1971). These studies show a considerable variation in heat transfer coefficient from the surface area between the ribs to the rib forward, top and aft surfaces. Most of the software tools for the design of cooling circuits in heat exchangers, however, have no provisions to handle either the geometric details of the ribs or the variations in heat transfer coefficients along the rib-roughened surface. Therefore, the cooling circuit designer is limited to assign an equivalent heat transfer coefficient on channel surface that accounts for the area enhancement, heat transfer coefficient variations and the rib fin effects. Heat transfer area enhancement is a purely geometric analysis that is presented in this paper for a verity of rib geometries. Variations in heat transfer coefficient on the area between the ribs (h_{floor}) and on the rib

surface itself (h_{rib}) are available for a wide range of rib geometries in open literature. Thus an area-weighted average heat transfer coefficient is easily evaluated for a wide range of rib geometries. This area-weighted average heat transfer coefficient, however, is based on the approximation that the entire rib surface is at the same temperature as the rib base, i.e., a 100% fin efficiency is assumed for the ribs. These ribs at the same time do not fall into the classical fin category for which the overall fin efficiencies are readily available. Therefore, the main adjective of this investigation was to generate a correlation for the rib fin effect corrections that encompasses all common rib geometric parameters as well as the common hot and cold side flow conditions.

2. DERIVATIONS

Consider the general case of a trapezoidal shape rib with round corners and fillets, mounted on a wall of a channel at an angle α with the flow direction as shown in Figure 1. A repeated computational domain will have a length of P (rib pitch) that includes a rib and half of the floor surface on each side of the rib.

a) Heat Transfer Areas for a Repeated Cell

The heat transfer areas for a typical repeated cell can be derived as:

$$A_{base}=[w_{bot}+2r_{fillet}\tan(\beta/2)]a/\sin(\alpha) \qquad \textbf{rib base (projection)} \tag{1}$$

$$A_{floor}=\{P-[w_{bot}+2r_{fillet}\tan(\beta/2)]/\sin(\alpha)\}a \qquad \textbf{surface area between a pair of ribs} \tag{2}$$

$$A_{rib}=\{2[(e/\sin\beta)-r_{top}\tan(\beta/2)-r_{fillet}\tan(\beta/2)]+[w_{top}-2r_{top}\tan(\beta/2)]+2(r_{top}+r_{fillet})\beta\}a/\sin(\alpha)$$
$$\textbf{rib exposed area} \tag{3}$$

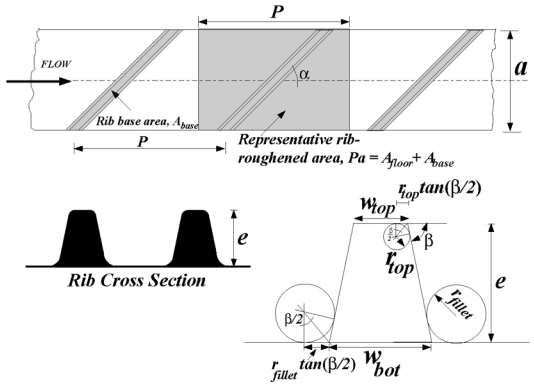

FIGURE 1. A typical rib geometry.

b) Rib Equivalent Heat Transfer Coefficient

The equivalent heat transfer coefficient for a rib is defined as a heat transfer coefficient that, when applied on the base surface of the rib (projection surface), will have the same thermal effects as that of the actual heat transfer coefficient applied on all rib exposed surfaces, i.e.

$$A_{rib}h_{rib} = A_{base}h_{equiv} \tag{4}$$

Substituting for these areas from Eqs. 1 through 3 and normalizing all rib dimensions with the rib height, e, we have

$$h_{equiv}=h_{rib}\{2[(1/\sin)-(r_{top}/e+r_{fillet}/e)\tan(\beta/2)]+[(w_{top}/e)-2(r_{top}/e)\tan(\beta/2)]+ 2\beta(r_{top}/e+r_{fillet}/e)\}/[(w_{bot}/e)+2(r_{fillet}/e)\tan(\beta/2)] \tag{5}$$

c) Overall Heat Transfer Coefficient

The overall heat transfer coefficient is the area-weighted average of the surface between a pair of ribs (floor) and the rib equivalent heat transfer coefficient, i.e.

$$A_{floor}h_{floor}+A_{base}h_{equiv}=h_{overall}(\mathrm{Pa}) \tag{6}$$

Where Pa is the projection area associated with one rib. Upon substitution for areas and heat transfer coefficients from Eqs. 1 through 5 with simplifications,

$$h_{overall}=h_{rib}\{2[(1/\sin\beta)-(r_{top}/e+r_{fillet}/e)\tan(\beta/2)]+[(w_{top}/e)-2(r_{top}/e)\tan(\beta/2)]+ 2\beta(r_{top}/e+r_{fillet}/e)\}/[(P/e)\sin\alpha]+h_{floor}\{(P/e)-[(w_{bot}/e)+2(r_{fillet}/e)\tan(\beta/2)]/\sin(\alpha)\}/(P/e) \tag{7}$$

Similarly, the overall Nusselt number and enhancement factor become:

$$\mathrm{Nu}_{overall}=\mathrm{Nu}_{rib}\{2[(1/\sin\beta)-(r_{top}/e+r_{fillet}/e)\tan(\beta/2)]+[(w_{top}/e)-2(r_{top}/e)\tan(\beta/2)]+ 2\beta(r_{top}/e+r_{fillet}/e)\}/[(P/e)\sin]+\mathrm{Nu}_{floor}\{(P/e)-[(w_{bot}/e)+2(r_{fillet}/e)\tan(\beta/2)]/\sin(\alpha)\}/(\mathrm{P/e}) \tag{8}$$

$$EF_{overall}=EF_{rib}\{2[(1/\sin\beta)-(r_{top}/e+r_{fillet}/e)\tan(\beta/2)]+[(w_{top}/e)-2(\mathrm{rtop/e})\tan(\beta/2)]+ 2\beta(r_{top}/e+r_{fillet}/e)\}/[(P/e)\sin\alpha]+EF_{floor}\{(P/e)-[(w_{bot}/e)+2(r_{fillet}/e)\tan(\beta/2)]/\sin(\alpha)\}/(P/e) \tag{9}$$

Equations 7, 8 and 9 can be simplified for a variety of special cases the results of which are presented in the appendix.

d) Correction for the Rib Fin Effects

In applying the h_{equiv} to the rib-roughened projection area on the cooling channel surface, it is assumed that the entire rib surface is at its base temperature. In other words, the rib fin effects are neglected. This assumption may not introduce any significant error for small blockage ratio ribs arranged at high pitch-to-height ratios. However, for high aspect and blockage ratio ribs, the error in the overall heat transfer coefficient can be as high as 20%.To investigate these effects, ten rib geometries (Fig. 5) were meshed and numerically analyzed for a range of pertinent parameters and realistic boundary conditions. The objective is to determine a correction factor that when is multiplied by h_{equiv}, it gives the final heat transfer coefficient, $h_{corrected}$, that can be directly applied to the projection area of the rib-roughened surface.

e) Numerical Models

Consider the configurations shown in Figure 2, representing a typical rib-roughened heat exchanger wall (on the left) and the simplified equivalent wall used in most thermal circuit design software tools (on the right). The total heat transfer rate per unit depth from the hot side to the cold side for the simple slab case is readily evaluated as:

$$\dot{Q}_{design} = \frac{P(T_{hot} - T_{cold})}{\frac{1}{h_{hot}} + \frac{t_{wall}}{k_{metal}} + \frac{1}{h_{corrected}}} = \frac{P(T_{hot} - T_{cold})}{R_{hot} + R_{wall} + R_{corrected}} \tag{10}$$

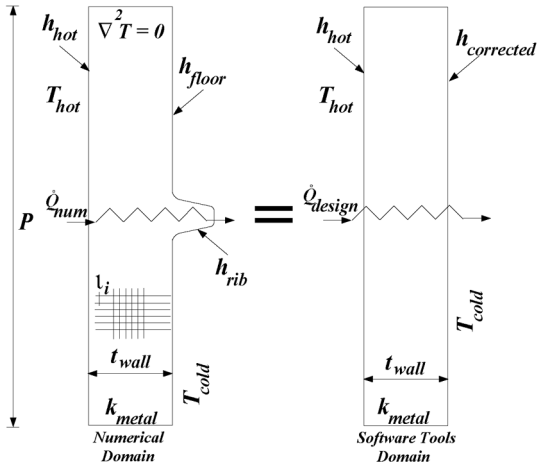

FIGURE 2. Equivalent thermal circuits.

The total heat transfer rate from the hot side to the cold side for the actual rib-roughened wall, however, was determined numerically. A typical mesh arrangement for a ribbed wall is shown in Figure 3. Taking advantage of the symmetry, only half of the domain, i.e., from the rib center to the floor center with a width of $P/2$ was mashed. A finite element package was used to solve the two-dimensional heat conduction equation, $\nabla^2 T = 0$, for the assigned convective boundary conditions on the gas and coolant sides and symmetric boundary conditions on the right and left boundaries where a rib-roughened wall repeats itself. The number of nodes and elements for a typical model were about 4700 and 4500, respectively. Temperature field for this geometry and for one set of assigned boundary conditions is shown in Figure 4. Once the temperature field was calculated, the total heat transfer rate from the hot side to the cold side was determined by:

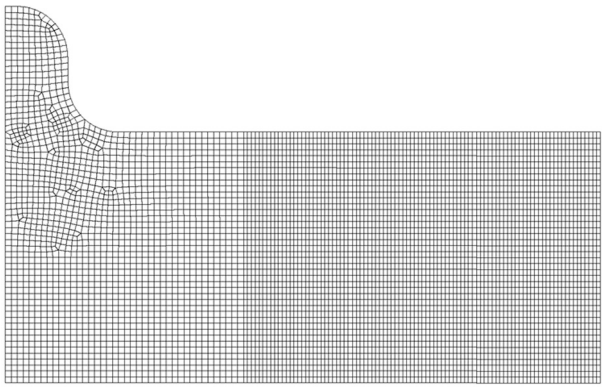

FIGURE 3. Mesh arrangement for a typical case.

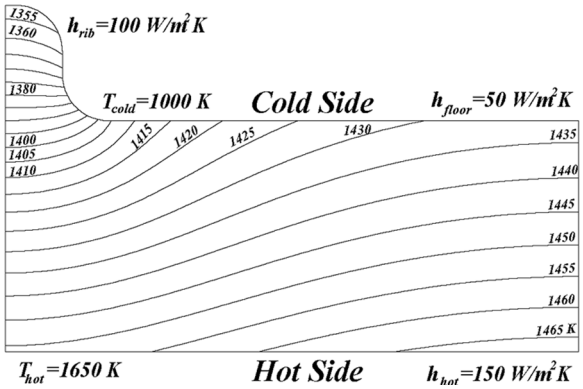

FIGURE 4. Temperature contours for a typical case.

$$\dot{Q}_{num} = h_{hot} \sum_{i=1}^{n} l_i (T_{hot} - T_{s,i}) \tag{11}$$

where n is the number of finite elements on the hot side of the numerical model and $T_{s,i}$ is the surface temperature of the i-th element on the hot side. Note that

$$\sum_{i=1}^{n} l_i = P$$

The corrected heat transfer coefficient was then calculated by equating Equations 10 and 11 to obtain $\dot{Q}_{design} = \dot{Q}_{num}$:

$$h_{corrected} = \frac{1}{\frac{P(T_{hot} - T_{cold})}{\dot{Q}_{num}} - (R_{hot} + R_{wall})} \tag{12}$$

The reported correction factor for the rib fin effect is defined as:

$$Correction\ Factor = \frac{h_{corrected}}{h_{overall}} = \frac{Nu_{corrected}}{Nu_{overall}} = \frac{EF_{corrected}}{EF_{overall}} \tag{13}$$

Figure 5 and Table 1 show all the geometries that were analyzed. Four rib aspect ratios (0.5, 1, 1.33, and 2) were investigated at four pitches to height ratios of 5, 7.5, 10 and 12.5. Each case was run for all sharp as well as round top corners and fillets.

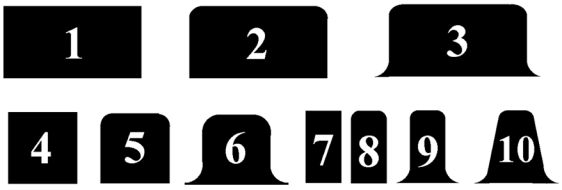

FIGURE 5. Analyzed rib geometries.

TABLE 1. Geometric specifications

AR_{rib}	P/e	r_{top}/e	r_{fillet}/e	$h_{rib\ (W/m2K)}$	$h_{floor\ (W/m2K)}$	*Geometry*
0.5	5, 7.5, 10, 12.5	0, 0.4	0, 0.4	88 - 212	22 - 88	1,2,3 Figure 5
1	5, 7.5, 10, 12.5	0, 0.4	0, 0.4	88 - 212	22 - 88	4,5,6 Figure 5
1.333	5, 7.5, 10, 12.5	0, 0.4	0, 0.4	88 - 212	22 - 88	10 Figure 5
2	5, 7.5, 10, 12.5	0, 0.4	0, 0.4	88 - 212	22 - 88	7,8,9 Figure 5
T_{cold}=1000 K, T_{hot}=1645 K, h_{hot}=141 W/m2K, k_{metal}=7.25 W/mK, t_{wall}=rib biggest dimension (height or width)						

3. RESULTS AND DISCUSSION

The first step in this investigation was to determine which parameters were dominant in rib fin effects. Earlier runs revealed that T_{cold}, T_{hot} and h_{hot} had little effects on the correction factor. The effects of t_{wall} and k_{metal} within the practical range of designs were also negligible. Therefore, these parameters were eliminated from the list of pertinent parameters. The following figures, representing a total of 386 runs, show the variation of the correction factor with respect to different parameters. They will help explaining how the process of collapsing all data points into a single curve was followed.

Figure 6 shows the variation of the correction factor with the hot side heat transfer coefficient, hhot, for the typical case of AR_{rib}=1, P/e=10 with round corners and fillets. Six cases for a range of hhot between 35 and 280 W/m^{2}K were run with no significant change in the correction factor. Figure 6 also shows the variation of the correction factor with (T_{hot} - T_{cold}) for the same typical case. Six cases for a range of (T_{hot} - T_{cold}) between 700 K and 1000 K (Thot was varied from 1450 K to 1650 K) were run with no significant change in the correction factor. It is also concluded from this figure that the correction factor is not affected by T_{hot} and T_{cold} individually. Other rib geometries showed similar behavior and, therefore, they are not reported here.

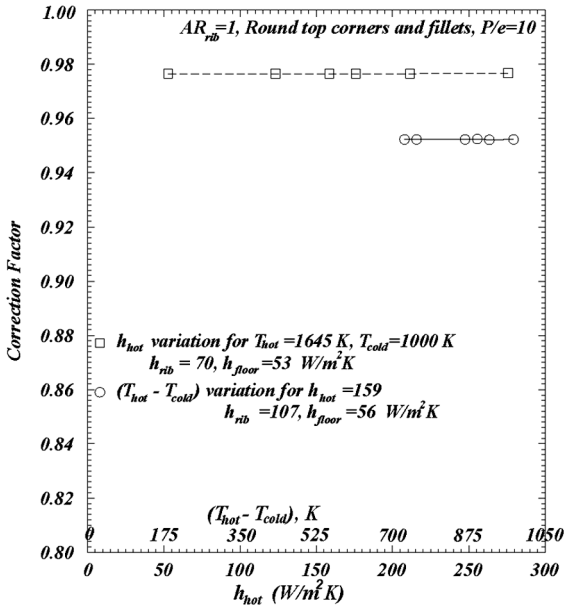

FIGURE 6. Correction factor variation with h_{hot} and with ($T_{hot} - T_{cold}$) for a rib aspect ratio of 1.

Figure 7 shows the variation of the correction factor with the rib pitch-to-height ratio, *P/e*, for three rib aspect ratios. Each rib geometry is run for three cases of all sharp corners, round top corners with no fillets and round top corners with fillets. The general trend is that the correction factor increases with *P/e* and with the rounding of top corners and presence of fillets for all cases. This behavior is expected since higher pitch-to-height ratios correspond to less number of ribs per given area and, as a result, lass rib fin effects on the overall heat transfer coefficient. Rib aspect ratio of 1 at *P/e*=12.5 has the highest correction factor while the rib aspect ratio of 2 at *P/e*=5 had the lowest correction factor.

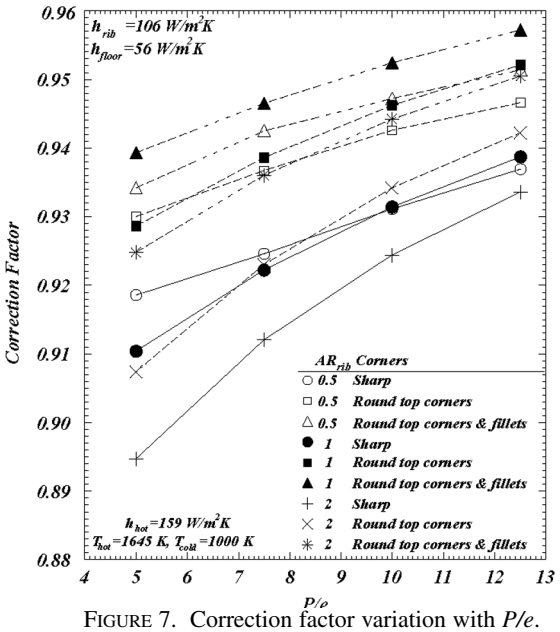

FIGURE 7. Correction factor variation with *P/e*.

Figures 8 through 11 show the variation of correction factor with h_{floor} and h_{rib} for four rib geometries representing three rectangular ribs with aspect ratios of 0.5, 1, and 2, and a trapezoidal case. The general behavior is the same for all these cases. The correction factor increases with hfloor and decreases with h_{rib}. A physical explanation for this behavior is that higher rib heat transfer coefficients correspond to higher convective heat transfer from the rib surface to the coolant and, as a result, higher temperature difference between the rib surface and rib base. Furthermore, the ribs with round corners and fillets produce higher correction factors then those of sharp corners and, as it was shown in Figure 7, the correction factor increases with the rib pitch-to-height ratio. It should be noted that a higher correction factor means that the rib surface temperature is less affected by the rib fin effect.

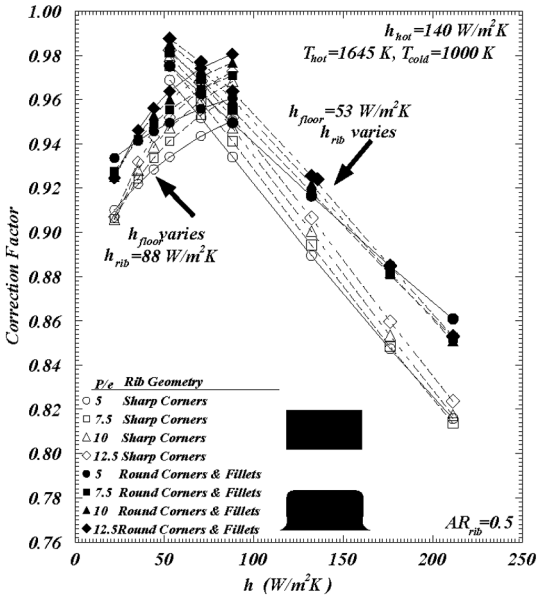

FIGURE 8. Correction factor variation with h_{rib} and with h_{floor} for a rib aspect ratio of 0.5.

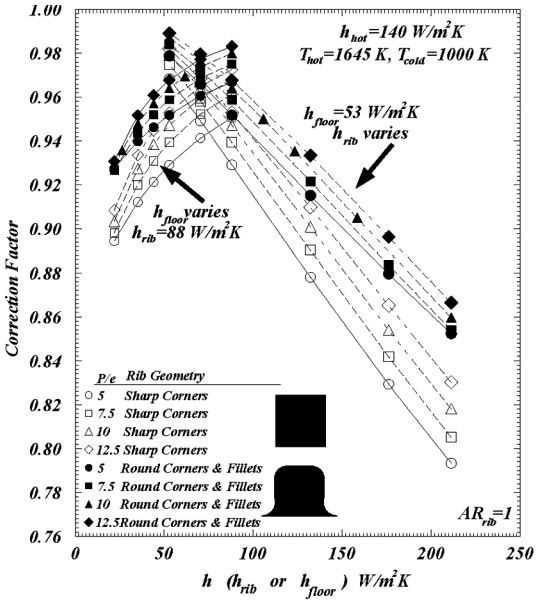

FIGURE 9. Correction factor variation with h_{rib} and with h_{floor} for a rib aspect ratio of 1.

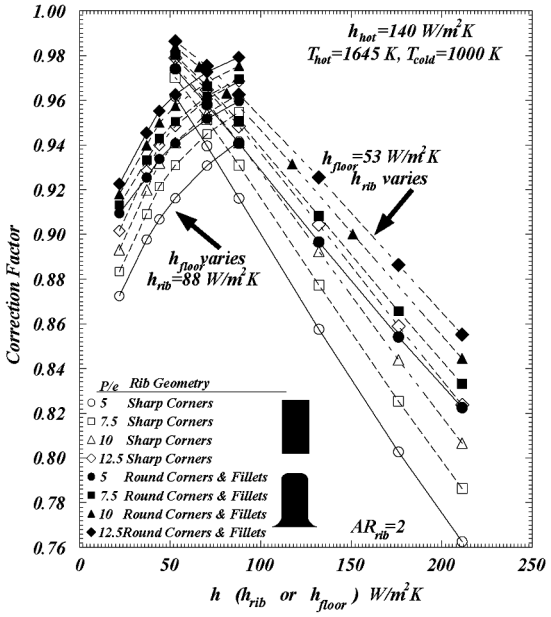

FIGURE 10. Correction factor variation with h_{rib} and with h_{floor} for a rib aspect ratio of 2.

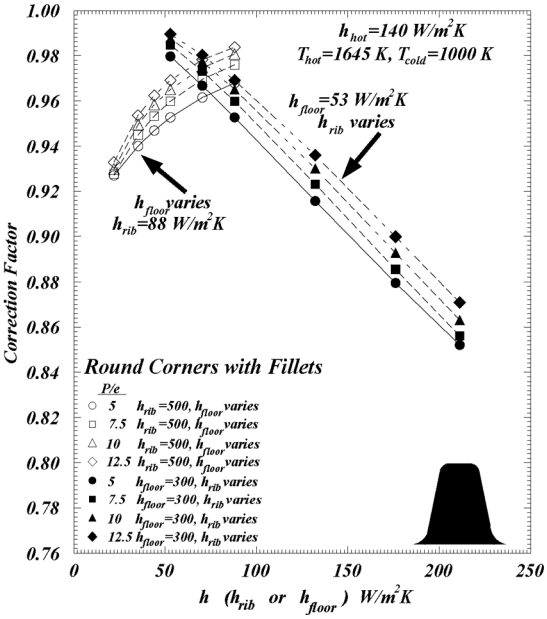

FIGURE 11. Correction factor variation with h_{rib} and with h_{floor} for the trapezoidal rib.

To get an idea about the overall range of the correction factor, all cases analyzed in this investigation are put together in Figure 12. High aspect ratio rib cases (AR_{rib}=2) with sharp corners have the lowest correction factor since, geometrically, they are closer to classical fins and, as a result, fin effects are more pronounced. The low aspect ratio rib cases especially with round corners and fillets have the highest correction factors, i.e. less fin effects since, geometrically, they are far from classical fins.

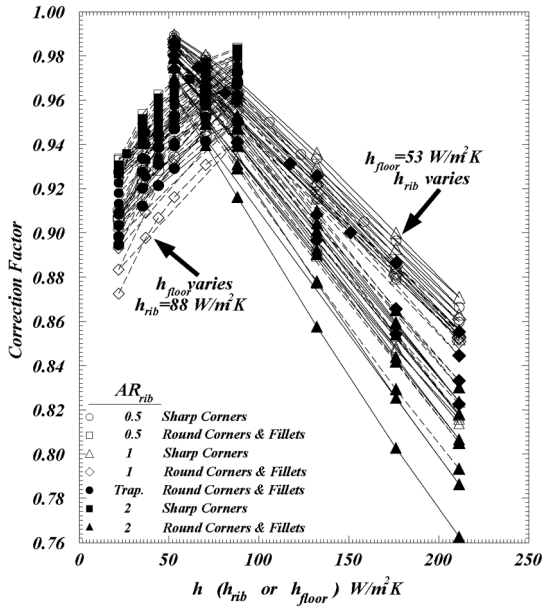

FIGURE 12. Correction factor variation with h_{rib} and with h_{floor} for all rib geometries.

The next major task was to find one non-dimensional group, comprised of all pertinent parameters affecting the correction factor, that when plotted against the correction factor, all data points collapse into one single curve. This was a trial and error process. Each individual parameter had to be looked at carefully to come up with an expression that closely represented its effect on the correction factor. For example, Figures 7 through 12 indicate that the correction factor is directly related to *P/e*, h_{floor} and corner radii while inversely related to h_{rib} and rib aspect ratio. With numerous iterations, the best non-dimensional parameter was determined to be:

$$x = \frac{h_{floor}^{0.8}}{h_{rib}^{2.2}} (P/e)^{0.6} \left[1 + \frac{\frac{r_{top}}{e}}{(\frac{P}{e})^{0.3}} \right] \left[1 + \frac{\frac{r_{fillet}}{e}}{(\frac{P}{e})^{0.3}} \right] \left| \sin(0.6\pi\, AR_{rib}) \right| \tag{14}$$

It should be noted that the trapezoidal rib results were best correlated when the rib aspect ratio in Equation 14 was set to unity although, based on the average of that rib top and bottom widths, one would calculate an aspect ratio of 1.333. Correction factor versus the non-dimensional parameter is shown in Figure 13. It can be seen that the results of the entire 386 cases correlate wall with the selected non-dimensional parameter. The final step was to apply the best-fit regression method to these data points. The results were the following three expressions, two linear for the lower and upper ends of the parameters and a sixth degree polynomial for the middle region, shown below:

$$y = 1947.7953x + 0.7156 \qquad (0 < x \leq 0.00007) \tag{15}$$

$$y = -7.5917.10^{18}x^6 + 2.4762.10^{16}x^5 - 3.23665.10^{13}x^4 + 2.17783.10^{10}x^3$$

$$-8.14111.10^{6}x^2 + 1.7577.10^{3}x + 0.76207 \qquad (0.00007 < x \leq 0.0008) \tag{16}$$

$$y = 12.89^4x + 0.9646 \qquad (0.0008 < x \leq 0.002) \tag{17}$$

where x is the non-dimensional parameter defined by Equation 14 and y is the correction factor due to rib fin effects.

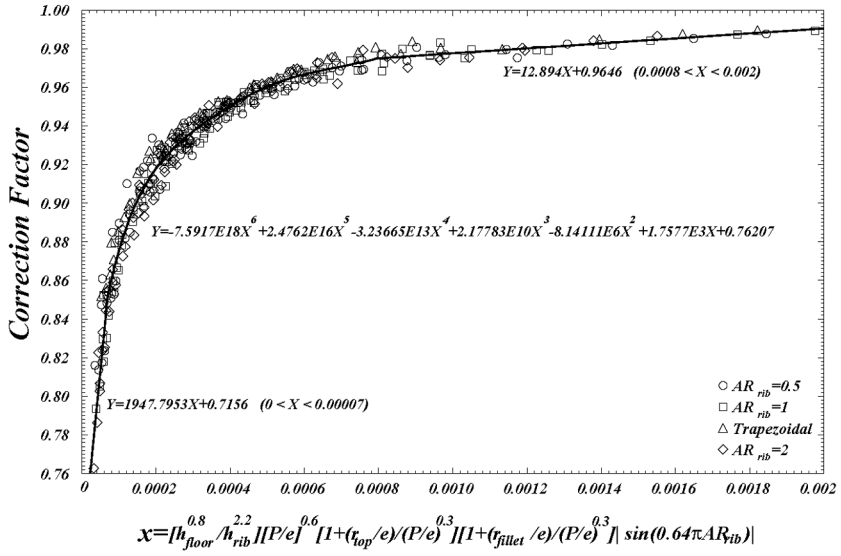

FIGURE 13. Correlated results for the correction factor of rib fin effects.

4. CONCLUSIONS

Major conclusions of this study were:

1) Rib fin effects should be taken into consideration in the design of heat exchangers and cooling circuits when, in using the software design tools, details of rib geometry and variations of heat transfer coefficients are replaced by an equivalent heat transfer coefficient and 2) while parameters such as h_{hot}, T_{hot} and T_{cold} play no significant role in rib fin effects, the rib geometry (rib aspect ratio, corner radii and pitch) as well as rib and floor heat transfer coefficients play an important role in rib fin effects on the overall rib-roughened surface heat transfer coefficient. A correlation for the correction of rib fin effects, encompassing all pertinent parameters is presented that can be conveniently used by the thermal circuit designers.

NOMENCLATURE

a	channel width (Figure 1)
A_{base}	rib base area (Figure 1)
A_{floor}	heat transfer area between two ribs
A_{rib}	rib total exposed heat transfer area
AR	channel aspect ratio
AR_{rib}	rib aspect ratio ($2e/(w_{top}+w_{bot})$)
D_h	channel hydraulic diameter
e	rib height
EF	enhancement factor, h/hsmooth=Nu/Nusmooth
$h_{correced}$	fin-effect-corrected heat transfer coefficient on a rib-roughened surface (Equation 12)
h_{equiv}	rib equivalent heat transfer coefficient (Equation 4)
h_{floor}	average heat transfer coefficient on the surface between a pair of ribs
h_{hot}	hot side average heat transfer coefficient
$h_{overall}$	overall area-weighted average heat transfer coefficient on a rib and on the surface between a pair of ribs
h_{rib}	average heat transfer coefficient on the rib surface
h_{smooth}	fully-developed heat transfer coefficient in a smooth channel
k_{metal}	rib-roughened wall thermal conductivity
l_i	finite element cell width on the gas side boundary
n	number of finite element cells on the gas side boundary
$\mathrm{Nu}_{corrected}$	fin-effect-corrected Nusselt number

$\mathrm{Nu}_{overall}$	overall area-weighted average Nusselt number on a rib and on the surface between a pair of ribs
Nu_{smooth}	Nusselt number for a fully-developed flow in a smooth channel
P	rib pitch (canter-to-canter)
Q_{design}	heat transfer from the hot side to the cold side calculated by the thermal design software tools (Figure 2)
Q_{num}	heat transfer from the gas to the coolant calculated from numerical models (Figure 2)
r_{fillet}	fillet radius
r_{top}	rib top corner radius
$R_{corrected}$	equivalent coolant side thermal resistance
R_{hot}	hot side thermal resistance
R_{wall}	rib-roughened wall thermal resistance
t_{wall}	rib-roughened wall thickness
T_f	film temperature
T_{cold}	cold side average temperature
T_{hot}	hot side average temperature
T_s	surface temperature
w_{top}	rib top width
w_{bot}	rib bottom width
x	non-dimensional parameter defined by Equation 14
y	correction factor defined by Equation 13
α	rib angle of attack
β	rib top angle (Figure 1)

REFERENCES

Abuaf, N., Gibbs, R. and Baum, R. 1986. Pressure Drop and Heat Transfer Coefficient Distributions in Serpentine Passages With and Without Turbulence Promoters. *The Eighth International Heat Transfer Conference*, Edited by C.L. Tien, V.P. Carey and J.K. Ferrel, 2837-2845.

Burggraf, F., 1970. Experimental Heat Transfer and Pressure Drop with Two Dimensional Turbulence Promoters Applied to Two Opposite Walls of a Square Tube. ASME, *Augmentation of Convective Heat and Mass Transfer*, Edited by A.E. Bergles and R.L. Webb, 70-79.

Chandra, P.R. 1987. Effect of Rib Angle on Local Heat/ Mass Transfer Distribution in a Two Pass Rib-Roughened Channel, Paper # 87-GT-94.

Chandra, P.R. and Han, J.C. 1989. Pressure Drop and Mass Transfer in Two-Pass Ribbed Channels. *J. Thermophysics & Heat Transfer*, Vol. 3, No. 3, 315-319.

Han, J.C., Glicksman, L.R. and Rohsenow, W.M. 1978. An Investigation of Heat Transfer and Friction for Rib Roughened Surfaces. *Int. J. Heat Mass Transfer*, Vol. 21, 1143-1156.

Han, J.C., 1984. Heat Transfer and Friction in Channels with Two Opposite Rib-Roughened Walls, *J. Heat Transfer*, Vol. 106, No. 4, 774-781.

Han, J.C., Perk, J.S. and Lei, C.K., 1985. Heat Transfer Enhancement Channels With Turbulence Promoters. *Journal of Engineering for Gas Turbines and Power*, Vol. 107, 628-635.

Han, J.C., Zhang, Y.M. and Lee, C.P. 1992. Influence of Surface Heat Flux Ratio on Heat Transfer Augmentation in Square Channels with Parallel, Crossed, and W-shaped Angled Ribs. *J. Turbomachinery*, Vol. 114, 872-880.

Korotky, G.J. and Taslim, M.E. 1997. Rib Heat Transfer Coefficient Measurements in a Rib-Roughened Square Passage. *J. Turbomachinery,* Vol. 120, No. 2, 376-385.

Liou, T.M., Hwang, J.J. and Chen, S.H. 1991. Turbulent Heat Transfer and Fluid Flow in a Channel with Repeated Rib Pairs. *Proc. ASME/JSME Thermal Eng*., Vol. 3, 205-212.

Liou, T.M. and Hwang, J.J. 1993. Effects of Ridge Shapes on Turbulent Heat Transfer and Friction in a Rectangular Channel. I*nt. J. Heat Mass Transfer*, Vol. 36, 931-940.

Metzger, D.E., Fen, C.S. and Pennington, J.W. 1983. Heat Transfer and Flow Friction Characteristics of very Rough Transverse Ribbed Surfaces With and Without Pin Fins. *Proc. ASME-JSME Thermal Engineering Joint Conference*, Vol. 1, 429-436.

Metzger, D.E, Chiu, M.K. and Bunker, R.S. 1988. The Contribution of On-Rib Heat Transfer Coefficients to Total Heat Transfer from Rib-Roughened Surfaces. *Transport Phenomena in Rotating Machinery*, Edited by J.H. Kim, Hemisphere Publishing Co.

Metzger, D.E., Fan, C.S. and Yu, Y. 1990. Effects of Rib Angle and Orientation on Local Heat Transfer in Square Channels with Angled Roughness Ribs. *Compact Heat Exchangers: A Festschrift for A.L. London*, Hemisphere Publishing Co., 151-167.

Taslim, M.E. and Spring, S.D. 1988. An Experimental Investigation of Heat Transfer Coefficients and Friction Factors in Passages of Different Aspect Ratio Roughened with 45o Turbulators. *Proc. National Heat Conference*, Houston, TX.

Taslim, M.E. and Spring, S.D. 1988. Experimental Heat Transfer and Friction Factors in Turbulated Cooling Passages of Different Aspect Ratios, Where Turbulators are Staggered. Paper # AIAA-88-3014.

Taslim, M.E. and Spring, S.D. 1994. Effects of Turbulator Profile and Spacing on Heat Transfer and Friction in a Channel. *J. Thermophysics & Heat Transfer*, Vol. 8, No. 3, 555-562.

Taslim, M.E., Li, T. and Kercher, D.M. 1996. Experimental Heat Transfer and Friction in Channels Roughened with Angled, W-Shaped, and Discrete Ribs on Two Opposite Walls. *J. Turbomachinery*, Vol. 118, 20-28.

Taslim, M.E. and Wadsworth, C.M. 1997. An Experimental Investigation of the Rib Surface-Averaged Heat Transfer Coefficient in a Rib-Roughened Square Passage. *J. Turbomachinery*, Vol. 119, 381-389.

Taslim, M.E. and Korotky, G.J.1998. Low-Aspect-Ratio Rib Heat Transfer Coefficient Measurements in a Square Channel. *J. Turbomachinery*, Vol. 120, 831-838.

Taslim, M.E. and Lengkong, A. 1998. 45o Staggered Rib Heat Transfer Coefficient Measurements in a Square Channel. *J. Turbomachinery*, Vol. 120, 571-580.

Taslim, M.E., Li, T. and Spring, S.D. 1998. Measurement of Heat Transfer Coefficients and Friction Factors in Passages Rib-Roughened on All Walls. *J. Turbomachinery*, Vol. 120, 564-570.

Taslim, M.E. and Lengkong, A. 1999. 45° Round-Corner Rib Heat Transfer Coefficient Measurements in a Square Channel. *J. Turbomachinery* , Vol. 121, 272-280.

Webb, R.L., Eckert, E.R.G. and Goldstein, R.J. 1971. Heat Transfer and Friction in Tubes with Repeated-Rib-Roughness. I*nt. J. Heat Mass Transfer*, Vol. 14, 601-617.

APPENDIX

Special Cases:

For certain applications, Equations 7, 8 and 9 are reduced to the following special cases :

1) Trapezoidal rib with round corners and fillets, perpendicular to flow direction (α=90°)

$$h_{overall}=h_{rib}\{2[(1/\sin\beta)-(r_{top}/e+r_{fillet}/e)\tan(\beta/2)]+[(w_{top}/e)-2(r_{top}/e)\tan(\beta/2)]+ 2\beta(r_{top}/e+r_{fillet}/e)\}/(P/e)+h_{floor}\{(P/e)-[(w_{bot}/e)+2(r_{fillet}/e)\tan(\beta/2)]\}/(P/e) \quad (18)$$

$$\mathrm{Nu}_{overall}=\mathrm{Nu}_{rib}\{2[(1/\sin\beta)-(r_{top}/e+r_{fillet}/e)\tan(\beta/2)]+[(w_{top}/e)-2(r_{top}/e)\tan(\beta/2)]+ 2\beta(r_{top}/e+r_{fillet}/e)\}/(P/e)+\mathrm{Nu}_{floor}\{(P/e)-[(w_{bot}/e)+2(r_{fillet}/e)\tan(\beta/2)]\}/(P/e) \quad (19)$$

$$EF_{overall}=EF_{rib}\{2[(1/\sin\beta)-(r_{top}/e+r_{fillet}/e)\tan(\beta/2)]+[(w_{top}/e)-(r_{top}/e)\tan(\beta/2)]+ 2\beta(r_{top}/e+r_{fillet}/e)\}/(P/e) + EF_{floor}\{(P/e)-[(w_{bot/e})+2(r_{fillet}/e)\tan(\beta/2)]\}/(P/e) \quad (20)$$

2) Rectangular rib with round corners and fillets, perpendicular to flow direction (α=90°, β=90°, $w_{top}=w_{bot}=w$)

$$h_{overall}=h_{rib}[2+(1/AR_{rib})-(4-\pi)(r_{top}/e)+(\pi-2)(r_{fillet}/e)]/(P/e)+h_{floor}\{1-[(1/AR_{rib})+ 2(r_{fillet}/e)]/(P/e)\} \quad (21)$$

$$\mathrm{Nu}_{overall}=\mathrm{Nu}_{rib}[2+(1/AR_t)-(4-\pi)(r_{top}/e)+(\pi-2)(r_{fillet}/e)]/(P/e)+\mathrm{Nu}_{floor}\{1-[(1/AR_{rib})+ 2(r_{fillet}/e)]/(P/e)\} \quad (22)$$

$$EF_{overall}=\mathrm{Nu}_{rib}[2+(1/AR_{rib})-(4-)(r_{top}/e)+(-2)(r_{fillet}/e)]/(P/e)+ EF_{floor}\{1-[(1/AR_{rib})+2(r_{fillet}/e)]/(P/e)\} \quad (23)$$

3) Rectangular rib with round top corners and no fillets, perpendicular to flow direction (α=90°, β=90° and r_{fillet}=0)

$$h_{overall}=h_{rib}[2+(1/AR_{rib})-(4-\pi)(r_{top}/e)]/(P/e)+h_{floor}\{1-[(1/AR_{rib})/(P/e)]\} \quad (24)$$

$$\mathrm{Nu}_{overall}=\mathrm{Nu}_{rib}[2+(1/AR_{rib})-(4-\pi)(r_{top}/)]/(P/e)+\mathrm{Nu}_{floor}\{1-[(1/AR_{rib})/(P/e)]\} \quad (25)$$

$$EF_{overall}=EF_{rib}[2+(1/AR_{rib})-(4-\pi)(r_{top}/)]/(P/e)+EF_{floor}\{1-[(1/AR_{rib})/(P/e)]\} \quad (26)$$

4) Rectangular rib with all sharp corners, perpendicular to flow direction (α=90°, β=90°, r_{top}=0 and r_{fillet}=0)

$$h_{overall}=h_{rib}[2+(1/AR_{rib})]/(P/e)+h_{floor}\{1-[(1/AR_{rib})/(P/e)]\} \quad (27)$$

$$\mathrm{Nu}_{overall}=\mathrm{Nu}_{rib}[2+(1/\mathrm{A}AR_{rib})]/(P/e)+\mathrm{Nu}_{floor}\{1-[(1/AR_{rib})/(P/e)]\} \quad (28)$$

$$EF_{overall}=EF_{rib}[2+(1/AR_{rib})]/(P/e)+EF_{floor}\{1-[(1/AR_{rib})/(P/e)]\} \quad (29)$$

5) Square rib with sharp corners, perpendicular to flow direction (α=90°, β=90°, r_{top}=0, r_{fillet}=0 and AR_{rib}=1)

$$h_{overall}=3h_{rib}/(P/e)+h_{floor}\{1-[1/(P/e)]\} \quad 30$$

$$\mathrm{Nu}_{overall}=3\mathrm{Nu}_{rib}/(P/e)+\mathrm{Nu}_{floor}\{1-[1/(P/e)]\} \quad 31$$

$$EF_{overall}=3EF_{rib}/(P/e)+EF_{floor}\{1-[1/(P/e)]\} \quad 32$$

Example:

Let us consider the case of e/D_h=0.167, AR_{rib}=1, P/e=8.5, =90°, r_{top}/e=0.25, r_{fillet}/e=0. For a typical Reynolds number of 15000, Korotky and Taslim (1997) report a rib Nusselt number of 166. The closest reported case for the heat transfer coefficient on the area between the ribs (h_{floor}) is the case of sharp corner ribs of the same blockage ratio at a pitch-to-height ratio of 10 by Taslim et. el (1996). Assuming that the sharp corner effects compensate for the higher pitch-to-height ratio, we use their reported Nusselt number of 110 for a Reynolds number of 15000. To calculate the correction factor due to rib fin effects, we need both h_{rib} and h_{floor}. For a D_h=7 mm cooling channel with a film temperature, T_f, of 1000 K and air thermal conductivity of 0.0027642 W/mK, the heat transfer coefficients are:

$h_{rib}=\mathrm{Nu}_{rib}k/D_h$= 60.9 W/m^{2}K and $h_{floor}=\mathrm{Nu}f_{loor}k/D_h$= 40.4 W/m^{2}K

Substituting these and other parameters in Equation 14, we will obtain a value of 0.000742 for the non-dimensional parameter x which, using Figure 13, gives a correction factor of 0.972 i.e. a 2.8% reduction in the overall heat transfer coefficient due to rib fin effects.